Osteoporosis International
https://doi.org/10.1007/s00198-022-06385-z

ORIGINAL ARTICLE

Lower limb bone geometry in adult individuals with X-linked hypophosphatemia: an observational study

Matteo Scorcelletti[1] · Serhan Kara[2] · Jochen Zange[2] · Jens Jordan[2] · Oliver Semler[3] · Eckhard Schönau[3] · Jörn Rittweger[2,3] · Alex Ireland[1] · Lothar Seefried[4]

Received: 7 December 2021 / Accepted: 25 March 2022

Abstract

Summary We assessed lower-limb geometry in adults with X-linked hypophosphatemia (XLH) and controls. We found large differences in multiple measures including femoral and tibial torsion, bowing and cross-sectional area and acetabular version and coverage which may contribute to clinical problems such as osteoarthritis, fractures and altered gait common in XLH.

Purpose Individuals with X-linked hypophosphatemia (XLH) are at risk of lower-limb deformities and early onset of osteoarthritis. These two factors may be linked, as altered biomechanics is a risk factor for osteoarthritis. This exploratory evaluation aims at providing clues and concepts for this association to facilitate future larger-scale and longitudinal studies on that aspect.

Methods For this observational study, 13 patients with XLH, aged 18–65 years (6 female), were compared with sex-, age- and weight-matched healthy individuals at a single German research centre. Femoral and hip joint geometry, including femoral and tibial torsion and femoral and tibial shaft bowing, bone cross-sectional area (CSA) and acetabular version and coverage were measured from magnetic resonance imaging (MRI) scans.

Results Total femoral torsion was 29° lower in individuals with XLH than in controls ($p < 0.001$), mainly resulting from lower intertrochanteric torsion (ITT) ($p < 0.001$). Femoral lateral and frontal bowing, tibial frontal bowing, mechanical axis, femoral mechanical–anatomical angle, acetabular version and acetabular coverage were all greater and tibial torsion lower in individuals with XLH as compared to controls (all $p < 0.05$). Greater femoral total and marrow cavity CSA, greater tibial marrow cavity CSA and lower cortical CSA were observed in XLH (all $p < 0.05$).

Discussion We observed large differences in clinically relevant measures of tibia and particularly femur bone geometry in individuals with XLH compared to controls. These differences may plausibly contribute to clinical manifestations of XLH such as early-onset osteoarthritis, pseudofractures and altered gait and therefore should be considered when planning corrective surgeries.

Keywords Bone · Femur · Geometry · Shape · XLH

✉ Lothar Seefried
l-seefried.klh@uni-wuerzburg.de

1 Research Centre for Musculoskeletal Science and Sports Medicine, Department of Life Sciences, Faculty of Science and Engineering, Manchester Metropolitan University, Manchester, UK

2 Division of Muscle and Bone Metabolism, Institute of Aerospace Medicine DLR, Cologne, Germany

3 Department of Pediatrics and Adolescent Medicine, University of Cologne, Cologne, Germany

4 Orthopaedic Department, University of Würzburg, Wurzburg, Germany

Introduction

X-linked hypophosphatemia (XLH) is a rare genetic disorder with an assumed incidence rate of 1 in 20,000 [1] caused by pathogenic variants in the phosphate regulating endopeptidase homolog, X-linked (PHEX) gene located at Xp22.1 [2]. The pattern of inheritance is X-chromosomal dominant with supposed complete penetrance. However, family history is negative in about one-third of cases, suggesting a relevant proportion of de novo mutations or an asymptomatic/undiagnosed parental status [3, 4]. By still not completely elucidated mechanisms, pathogenic, loss-of-function variants in PHEX lead to elevated levels of the phosphatonin fibroblast

Published online: 18 April 2022

growth factor 23 (FGF-23). Resulting renal phosphate wasting and compromised production of 1,25 dihydroxyvitamin D along with further disease mechanisms cause a wide spectrum of clinical manifestations [5]. Specifically, skeletal issues including short stature and limb deformities, joint problems and early-onset osteoarthritis are a universal finding in almost all patients [2, 6–9]. Common deformities of the weight-bearing lower limbs in XLH comprise abnormal diaphyseal bowing and torsion including unphysiological femoral torsion (alternatively known as femoral neck anteversion or FNA) [7, 10]. These deformities have clinical relevance, as differences in joint geometry likely contribute to increased risk of (pseudo-)fractures [11–13] and impaired joint congruity both directly through altered biomechanics and indirectly through effects on muscle tractive forces and gait in individuals with XLH [8, 14]. In addition to direct effects of PHEX deficiency and elevated FGF-23 on mineral metabolism and skeletal development, other disease-associated manifestations such as delayed motor development [9, 15] and greater incidence of childhood obesity in children with XLH [16] likely contribute to differences in joint development and wearing [17, 18]. Moreover, hip joint geometry has been identified to have predictive value with regards to developing osteoarthritis independent of clinical risk factors [19] and recent analyses highlight that specifically femoral torsion, on the one hand, is influenced by mechanical loading and, on the other, can contribute to osteoarthritis development [13].

While the incidence of skeletal deformities in XLH has been reported according to clinical assessment thresholds or by self-report [9, 20], an objective characterization of bone geometry in adults with XLH has not been completed. Therefore, we assessed multiple components of lower-limb geometry in individuals with XLH, and compared them to those in an age- and sex-matched control group. We hypothesized that we would observe altered joint geometry in individuals with XLH.

Methods

Cohort

Evaluations are based on data obtained from an exploratory clinical study comparing 13 patients with X-linked hypophosphatemia (XLH) and 13 unaffected, age-, sex- and weight-matched controls. Per selection criterion, participants were 18–65 years old and did not have any acute disorders or conditions that would interfere with planned assessments.

For all XLH subjects, genetic confirmation of the diagnosis was available. Data regarding their previous medical and surgical treatment was based on medical history. Accessible information included age at initiation of medical treatment and number of surgeries to the leg under consideration and is provided in Suppl. 1. Considering patients' age and the fact that most treatments were initiated in childhood, written documentation and medical records regarding dosage over time and formulations of substitutional treatment or technical details regarding surgeries could not be reproduced by the participants. Control group participants were recruited among patients' friends and spouses who did not have any bone disease, bone targeted medication nor a history of corrective surgery to the evaluated leg.

While the core study is intended to comparatively evaluate muscle fatigue and physical performance in XLH vs healthy controls, data presented here is dedicated to a subanalysis of an MRI data–based evaluation of leg and hip geometry. Height and body mass were recorded.

Magnetic resonance imaging scan parameters

In this study, 5 sets of 64 transverse images each were recorded from the right leg and body side reaching at least from the foot to the lower part of the lumbar spine using a 3-T Siemens Biograph. Images were recorded using a turbo 2 echo DIXON sequence with the following parameters: flip angle 10°, TR 7.02 ms, TE1 2.46 ms, TE2 3.69 ms, 300 mm × 300 mm field of view at 1.2 mm × 1.2 mm × 4 mm voxel size. In this study, only images covering the region of the femur and tibia were evaluated.

Image analysis

MRI images were analysed using ImageJ (Version1.52 h). The total femoral torsion was defined using the femoral neck line and the posterior condylar line. The femoral neck line was defined as the line between the femoral head centre, and the shaft centre directly distal to the lesser trochanter. The posterior condylar line was defined as the line joining the posterior apices of the condyles in the image where the condyles were most prominent.

The inter-trochanteric torsion (ITT) was defined as the angle between the femoral neck line and the lesser trochanter line. The lesser trochanter line was defined as the line between the apex of the lesser trochanter at peak lesser trochanter size and the shaft centre. The shaft torsion (ST) is the angle between the lesser trochanter line and the posterior distal shaft line, which is aligned with the flat posterior distal shaft surface immediately proximal to the posterior condyles. The condylar torsion (CT) is the angle between the posterior distal shaft line and the posterior condylar line (Fig. 1). Tibial torsion was measured by the angle of the posterior tibial condylar line as reference and the line connecting the medial and lateral malleoli. The angle will be negative when the distal tibia rotates externally respective to the proximal tibia.

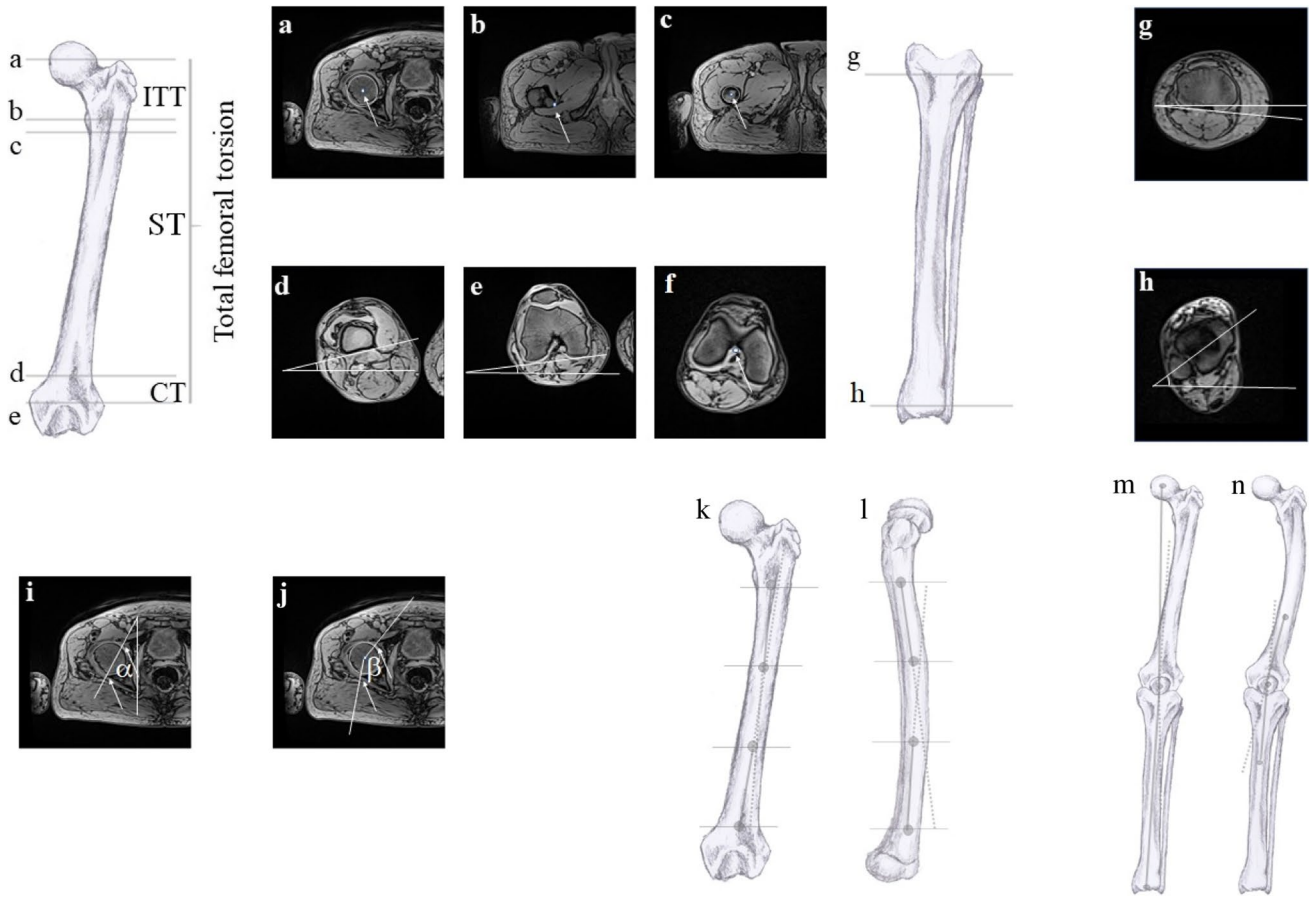

Fig. 1 Angle definitions: **a** femoral head centre, **b** apex of lesser trochanter, **c** shaft centre, **d** posterior distal shaft line, **e** posterior condylar line, **f** intercondylar notch, **g** posterior tibial condylar line and **h** lateral and medial malleoli. **i** Acetabular version α. **j** Acetabular coverage angle β. The slice where the circumference of the femoral head was largest was chosen for analysis. The arrows show the rim of the acetabulum. **k** Femoral lateral bowing landmarks. **l** Femoral frontal bowing landmarks. **m** Mechanical axis landmarks. **n** femorotibial angle landmarks. Illustrations by X. O'Reilly-Berkeley

To measure femoral lateral and frontal bowing, the shaft centre was identified at four landmarks: immediately distal to the lesser trochanter, at 1/3 proximal–distal femoral shaft length; at 2/3 proximal–distal femoral shaft length (shaft is between slice "c" and "d" in Fig. 1) and at the femoral intercondylar notch. Likewise, tibial lateral bowing and frontal bowing were defined using the shaft centre at the intercondylar notch, the proximal third of the tibia and the distal third of the tibia at the distal tibial plateau.

The two lines used to define the mechanical axis are those connecting the femoral head centre to the femoral intercondylar notch, and from the midpoint of the tibial intercondylar eminence to the midpoint of the distal tibial epiphysis. The two lines defining the femorotibial angle were those connecting the femoral shaft centre at the distal third of the femur and the intercondylar notch, and the intercondylar notch and the proximal third of the tibia. Lastly, the femoral mechanical–anatomical angle is defined by the lines connecting the femoral head centre to the intercondylar notch and the intercondylar notch to the centre of the femur immediately distal to the lesser trochanter.

The acetabular version was assessed in the cross section where the femoral head was greatest. It was defined as the angle between the anterior and posterior acetabular margins of the acetabulum and the sagittal plane (Fig. 1). On the same slice, the acetabular coverage was assessed as the angle between the posterior margin of the acetabulum and the femoral head centre and the anterior margin of the acetabulum and the femoral head centre.

To calculate the relevant angle λ in the frontal plane, the coordinates of the desired landmarks were calculated using the formula:

$$\lambda = \arctan\left(\frac{\frac{ay-by}{ax-bx} - \frac{cy-dy}{cx-dx}}{1 - \frac{ay-by}{ax-bx} * \frac{cy-dy}{cx-dx}}\right)$$

where *a* and *b* represent the respectively the proximal and distal reference points of the proximal axis and *c* and *d* the proximal and distal reference points of the distal axis. *b* and *c* overlap in the case of the mechanical axis and femorotibial angle (Fig. 1). *y* and *x* on the other hand are respectively the antero-posterior coordinates and the medio-lateral coordinates.

Statistical analysis

Femoral and tibial geometry, femorotibial alignment and acetabular parameters were compared in individuals with XLH and in control participants. Data from both groups were tested for normal distribution with the Shapiro–Wilk test. Parametric data were expressed as mean ± SD, non-parametric data as median and interquartile range (IQR).

For parametric data, homogeneity of variance was checked with Levene's test and the Student t-test was implemented to assess group differences. For non-parametric data, the Mann–Whitney U test was applied to test for group differences. Repeatability of the measures performed has been calculated using SPSS statistical package version 23 (SPSS Inc, Chicago, IL) by the intraclass correlation coefficient (ICC). It was calculated based on a mean rating of the 3-image analysis as well as absolute effects, using a 2-way mixed-effect model to assess the repeatability of the image analysis by the same examiner at three different times in random order [21]. ICC was found to be excellent for total femoral torsion (ICC: 0.989), ITT (ICC: 0.968), femoral lateral bowing (ICC: 0.978), femoral frontal bowing (ICC: 0.904), tibial torsion (ICC: 0.93), tibial lateral bowing (ICC: 0.938), mechanical axis (ICC: 0.958) and femoral mechanical–anatomical angle (ICC: 0.974). Values for CT (ICC: 0.843), tibial frontal bowing (ICC: 0.768), acetabular version (ICC: 0.859) and acetabular coverage (ICC: 0.855) showed good reliability.

Results

Out of 13 subjects enrolled per group, whole-leg MRI imaging could be evaluated from 11 individuals with XLH (mean age 48.7 ± 9.2 years, 6 female, 77.3 kg) and 13 age-, sex- and weight-matched controls (mean age 48.8 ± 7.6 years, 6 female, 79.9 kg, $p > 0.677$). The mean height of the XLH individuals was 1.56 m, and the control group height was 1.69 m (Table 1). For two male patients in the XLH group, MRI data could not be analysed due to extensive artefacts from metal implants.

Both basic characteristics and each of the measured angles were normally distributed apart from tibial frontal bowing. Individuals with XLH and control participants had similar age, body mass and BMI although control participants were taller than individuals with XLH ($p = 0.006$).

Table 1 Mean, standard deviation (SD) and group comparison *p*-values for descriptive variables of the studied groups. BMI: body mass index

Variable	XLH ($n = 11$) 5 male/6 female		Control ($n = 13$) 7 male/6 female		*t*-test
	Mean	*SD*	*Mean*	*SD*	*p-value*
Age (years)	48.7	9.2	48.8	7.6	0.995
Height (m)	1.56	0.10	1.68	0.09	0.006
Weight (kg)	77.3	16.5	79.9	13.2	0.677
BMI (kg/m^2)	32.0	8.5	28.4	4.6	0.223

The total femoral torsion in the XLH group was 8.4 ± 20.2° and thus significantly lower than in the control group with 37 ± 14.2° ($p < 0.001$; Fig. 2). When evaluating regional torsion on different levels along the femoral axis, group differences in femoral torsion appeared to primarily result from significantly lower inter-trochanteric torsion (ITT) in the XLH group with 36.4 ± 12.3° as compared to the control group with 54.9 ± 9.5° ($p < 0.001$), as well as a lower condylar torsion (CT) in in XLH vs control with 1.5 ± 5.3° vs 7.2 ± 2.9°, respectively ($p < 0.005$; Fig. 2). In contrast, the shaft rotation or shaft torsion (ST) was similar in both XLH patients (− 29.5 ± 17.9°) and controls (− 26.3 ± 12.05°) ($p = 0.620$). The tibia was less externally rotated in individuals with XLH − 8.7 ± 13.5° than in the control group − 37.2 ± 11.8° ($p < 0.001$).

Substantial between-group differences were also evident regarding limb bowing. Femoral bowing was significantly enhanced in individuals with XLH vs controls for both lateral bowing with 13.1 ± 7.0° vs -1.0 ± 2.5° ($p < 0.001$), as well as frontal bowing with 31.4 ± 7.3° vs 17.8 ± 1.4° ($p < 0.001$), respectively.

There was no apparent difference in tibial lateral bowing, whereas for tibial frontal bowing (which was not normally distributed) the median value of 11.6° (IQR 7.8°, 19.5°) for individuals with XLH was higher than that in controls 5.0° (IQR: 2.9°–7.7°, $p < 0.005$; Fig. 3).

In terms of lower-limb alignment, there was an enhanced valgus of the mechanical axis in the XLH group (5.6 ± 5.3°) as compared to the control group (1.5 ± 2.5°, $p < 0.05$) In contrast, the average femorotibial angles were not significantly different between the groups. Accordingly, there was a significant difference in the femoral mechanical–anatomical angle, representing the difference between the mechanical and anatomical axis. In that regard, the average femoral mechanical-anatomical angle was 9.1 ± 2.2° in the XLH group and only 5.1 ± 0.8° in controls ($p < 0.001$; Fig. 4).

Acetabular version was significantly increased in individuals with XLH (23.6 ± 8.4°) as compared to those in

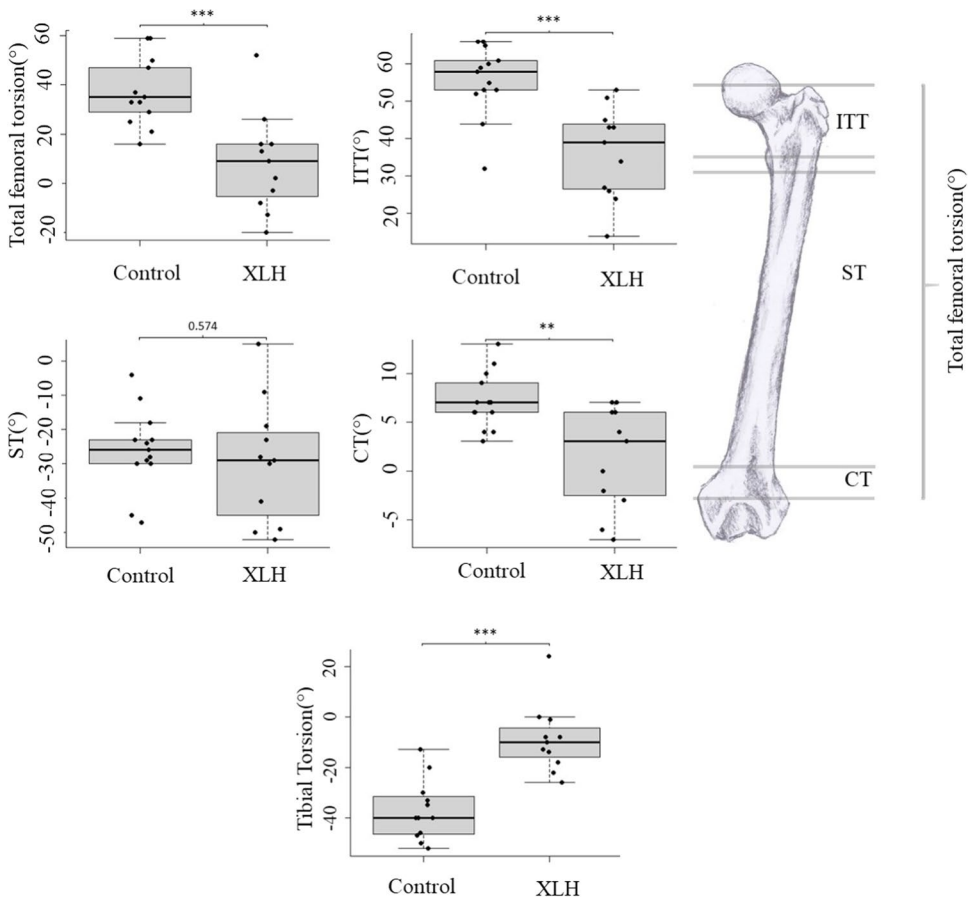

Fig. 2 Total and regional torsion of the femur compared between control participants and individuals with XLH. Boxplots indicate median, interquartile range, minimum and maximum values. Femoral torsion, ITT—intertrochanteric torsion, ST—shaft torsion, CT—condylar torsion. Positive degrees represent external torsion from the frontal plane. Asterisks indicate results of group comparisons—*$p<0.05$, **$p<0.01$, ***$p<0.001$. Illustrations by X. O'Reilly-Berkeley

the control group (17.5 ± 3.9°, $p<0.05$). Additionally, acetabular coverage was 32.6° higher in individuals with XLH (192.5 ± 22.6°) than in the control group (159.9 ± 9.1°, $p<0.001$; Fig. 5).

The total CSA of the femoral head and at the lesser trochanter showed no differences between the two groups. The total CSA of femoral shaft sites was ~ 21–24% greater in individuals with XLH compared to the control group ($p<0.015$). The bone marrow cavity of the femoral shaft sites was also greater in XLH individuals (all $p<0.05$), such that the cortical bone area was similar between groups. The total CSAs of the three tibial shaft sites and the talus were similar between the groups. The bone marrow cavities of the proximal and mid-tibial shaft sites were greater ($p<0.05$) and cortical CSAs at all shaft sites lower ($p<0.05$ except proximal sites $p=0.069$) in the XLH individuals compared to the control subjects (Table 2).

Discussion

This study was the first to objectively characterise and compare multiple components of lower-limb bone geometry between individuals with XLH and controls. We observed considerable differences in multiple clinically relevant aspects, largely in line with previous clinical and self-reports [9, 14]. Specifically, individuals with XLH exhibited significantly lower femoral torsion as compared to controls. Further detailed analysis revealed this difference to result mainly from a lower proximal, intertrochanteric torsion. While lower distal condylar torsion also appeared to contribute, no group differences in shaft torsion were evident. In that regard, one may speculate that this could be due to enhanced torsional strain towards the joint, i.e. at the intertrochanteric and the condylar area. However, other clinical populations have shown different contributions of subtrochanteric and supertrochanteric torsion to total femoral torsion [22]. This is clinically important, as when pharmacological treatment during growth to prevent femoral deformities has failed and femoral osteotomy is considered [23], it is important to correct torsion in the correct region [13, 22]. To date, surgical protocols focus on frontal plane deformations [7, 24, 25]; therefore, assessment of femoral torsion should also inform development of future guidelines. Furthermore, characterising the overall lower limb geometry of this clinical group could inform about possible sources of joint incongruity, fractures, osteoarthritis and gait disturbances other than frontal plane deformations.

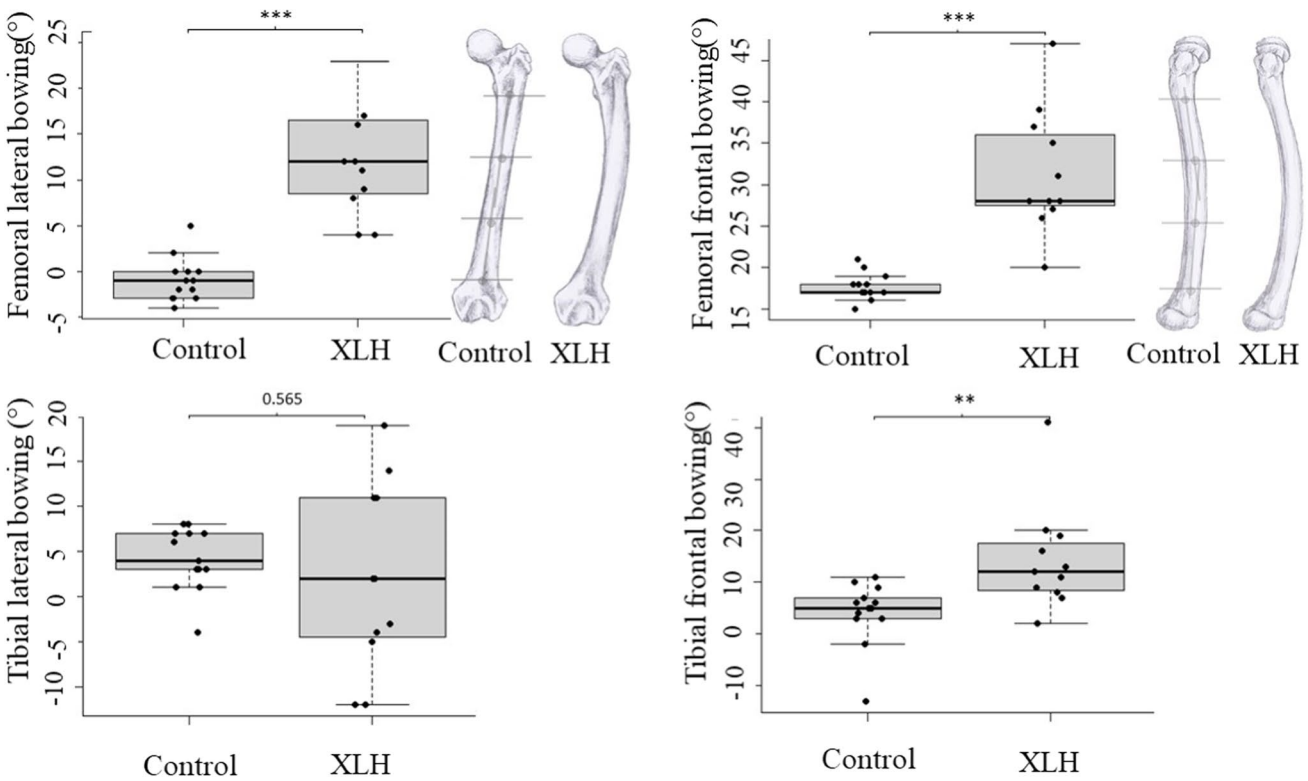

Fig. 3 Femoral and tibial bowing in the two groups; positive values indicate anterior and lateral bowing. Boxplots indicate median, interquartile range, minimum and maximum values. $*p<0.05$, $**p<0.01$, $***p<0.001$. The illustration in the top left panel shows a visual representation of the average difference between the two groups from a frontal view. On the control panel, the method of the bowing's measurement is drawn on. The illustration in top right panel shows the average difference from a lateral view. Illustrations by X. O'Reilly-Berkeley

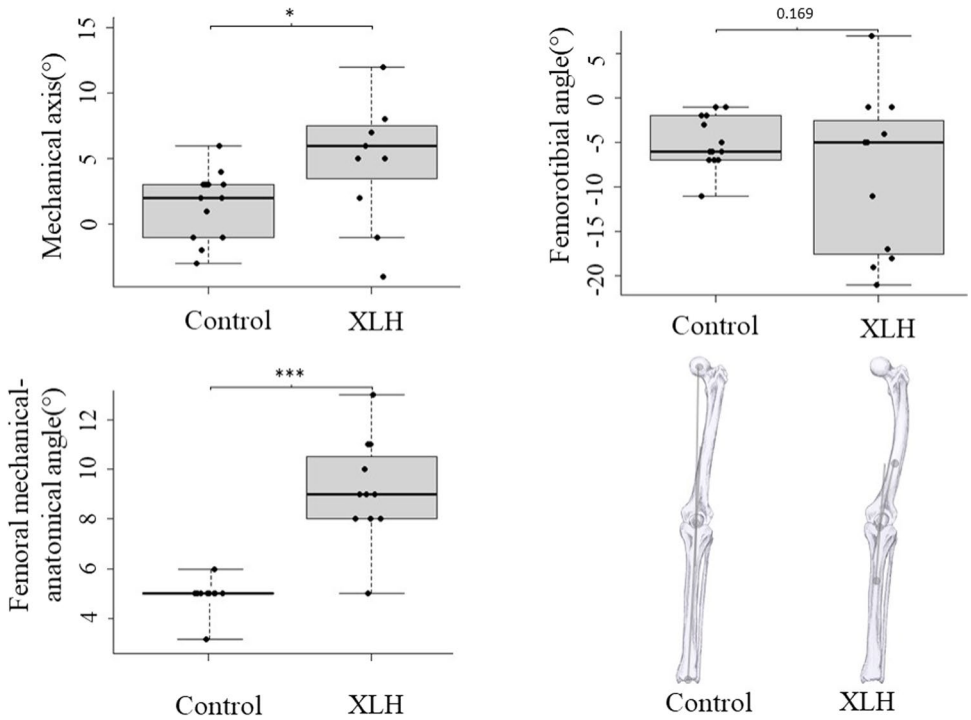

Fig. 4 Mechanical axis, femorotibial angle and femoral mechanical–anatomical angle in the two groups. Boxplots indicate median, interquartile range, minimum and maximum values. Positive degrees are outward lateral. $*p<0.05$, $**p<0.01$, $***p<0.001$. The bottom right panel shows the visual representation of lower-limb alignment. Also, the mechanical axis is drawn on the control limb and the femorotibial angle on the XLH limb. Illustrations by X. O'Reilly-Berkeley

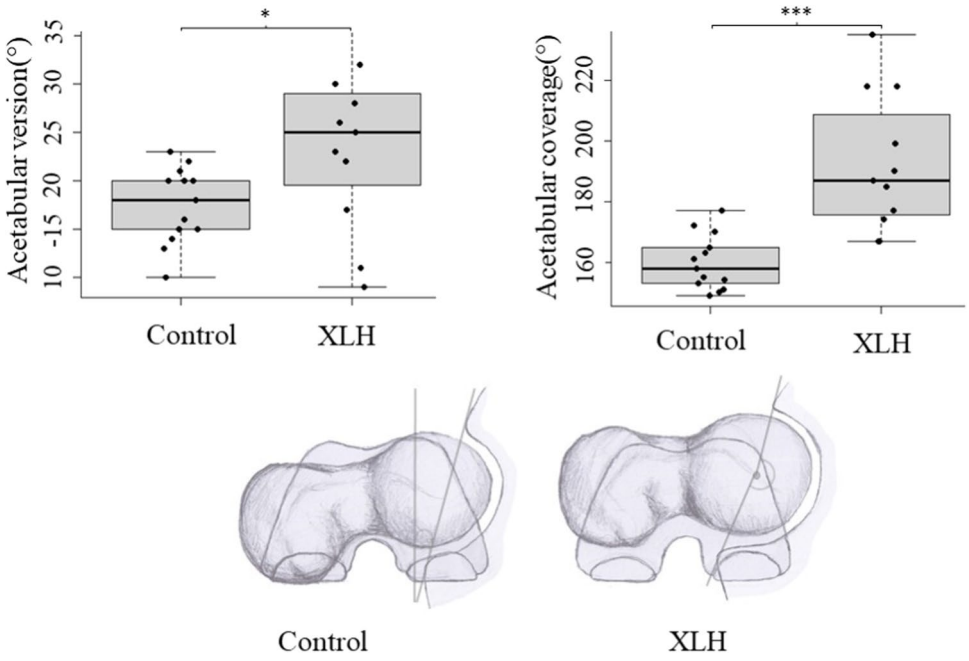

Fig. 5 Acetabular version and acetabular coverage for the two groups. For the acetabular version, positive values indicate anterior rotation from a lateral position, for the acetabular coverage values indicate the portion of the femoral head within the acetabulum. Boxplots indicate median, interquartile range, minimum and maximum values. $*p<0.05$, $**p<0.01$, $***p<0.001$. The bottom panel shows a visual representation of the acetabular geometry, the femoro-acetabular relationship and the total femoral torsion with the outline of the knee in the background. On the control panel, the acetabular version measurement is drawn on, and on the XLH panel we can see the acetabular coverage measurement. Illustrations by X. O'Reilly-Berkeley

Moreover, we observed significantly increased acetabular coverage of the hip joints in the XLH cohort. This is particularly important since both reduced femoral torsion and increased acetabular coverage are known to predispose to hip osteoarthritis development [26]. Conversely, a recent large study in a Caucasian population with end-stage knee osteoarthritis [27] revealed a correlation between increasing coronal valgus alignment and increased external condylar torsion as well as increased tibial torsion while in our XLH cohort, coronal valgus deformity correlated with decreased condylar torsion and decreased tibial torsion, suggesting that mechanisms of knee osteoarthritis in XLH might differ from what is observed in the general population. These findings may be important contributions to better understand early osteoarthritis development in XLH [8, 28]. Moreover, it is important to keep in mind that increased acetabular coverage and diminished ITT as the main contributor to low femoral torsion are not directly affected by corrective surgeries in XLH, usually addressing the diaphyseal/distal femur and the proximal tibia. Along the diaphyseal segment, we observed increased frontal and lateral bowing in the XLH cohort at the femur, while differences concerning bowing of the tibia were less pronounced and only significant with regards to frontal bowing. Finally, there was lower external rotation of the tibia (tibial torsion) in line with previous reports [7].

There was larger inter-individual variation for most aspects of skeletal geometry in people with XLH, and the causes and consequences for this need to be identified. The above results agree with current qualitative literature about deformities in patients with XLH [7, 25, 29]; however, detailed quantification of limb geometry in this clinical group was not yet available in the literature.

The observation of a significantly greater total cross-sectional area of the femur is remarkable, considering the overall reduced body size of XLH patients as compared to controls. This is in line with a previous peripheral quantitative computed tomography (pQCT) study in tibia in children and adults (age 23 ± 13 years) with XLH [30]. Looking at it more closely, the difference results from an enlarged marrow cavity on all height levels along the femoral axis while the cortical cross-sectional area is not significantly different on these levels. In contrast, the generally larger tibia marrow cavity in the absence of a pronounced advantage in total CSA in XLH resulted in lower cortical CSA throughout tibia length. One may speculate if the pronounced femoral hypertrophy results from childhood rickets with compromised bone quality and deficient mineralization leading to enhanced mechanical strain and increased bone turnover with intensified endosteal bone resorption and periosteal apposition.

Table 2 Cross sectional area (CSA) of femur and tibia at multiple locations. Where the marrow cavity was not present, only total CSA has been evaluated. CSA is outlined in mm^2. In the % column, we show the difference between XLH and control in percentage with the control group as reference. Bottom panel, visual representation of femur CSA on the left, and tibial CSA on the right. Illustrations by X. O'Reilly-Berkeley

Bone	*Site*		*Total CSA*						*Bone marrow CSA*						*Cortical bone CSA*					
			XLH		Control				XLH		Control				XLH		Control			
			mean	*SD*	*mean*	*SD*	*%*	*p*	*mean*	*SD*	*mean*	*SD*	*%*	*p*	*mean*	*SD*	*mean*	*SD*	*%*	*p*
Femur	Head centre		1840	274	1923	303	-4	*0.559*												
	Under lesser trochanter		1093	223	966	159	13	*0.182*												
	Shaft	Proximal 3rd	823	132	674	104	22	***0.015***	389	116	172	39	126	***<0.001***	431	117	502	75	-14	*0.147*
		Middle	829	137	671	100	24	***0.011***	355	128	203	64	75	***0.004***	452	138	468	67	-3	*0.752*
		Distal 3rd	853	202	703	108	21	*0.062*	382	54	312	72	22	***0.042***	487	180	391	59	25	*0.136*
	Distal flat shaft		1790	277	1551	174	15	***0.039***												
Tibia	Shaft	Proximal 3rd	701	144	670	93	5	*0.592*	439	92	344	73	28	***0.026***	262	87	326	50	-20	*0.069*
		Middle	526	86	516	75	2	*0.79*	278	81	164	28	70	***<0.001***	247	61	351	66	-30	***0.003***
		Distal 3rd	460	78	469	136	-2	*0.881*	214	60	158	124	35	*0.254*	246	57	310	44	-21	***0.014***
	Talus		1755	220	1618	230	8	*0.221*												

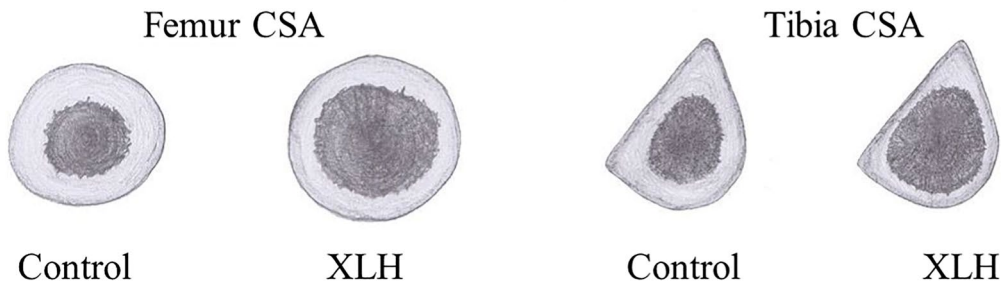

Overall, there are likely a number of factors which contribute to the observed findings. Fundamentally, the osteoid content of subjects with osteomalacia results in higher ductility of the bone structure [31]. This abnormality likely leads to changes in deformation patterns caused by mechanical loading during daily activities and exercise, in addition to the resultant adaptive response in bone geometry. In addition, increased bone ductility may also underlie the higher acetabular coverage due to the pressure of the femoral head on the acetabulum. Altered bone composition and mechanical loading may also contribute to the greater variance observed in the group with XLH. In relation to mechanical loading, XLH is associated with muscle weakness [32] and altered gait [8, 14] which likely result in altered bone loading. In a similar vein, childhood motor development, which has been shown to affect development of bone geometry [33, 34], is delayed in children with XLH [35].

These results have both functional and clinical implications for individuals with XLH. Waddling gait and early osteoarthritis at weight-bearing joints are commonly diagnosed in individuals with XLH [7, 8, 14]. In particular, the high prevalence of osteoarthritis in up to 55% even in individuals under the age of 30 is of particular concern [9, 36]. Also, altered femoral geometry likely contributes to the high prevalence of lower limb and specifically femoral pseudo-fractures in XLH [37]. Femoral torsion and proximal femur varus deformities have been shown to change the lever arms of hip muscles and therefore decrease hip muscle strength [22, 38, 39]. This alteration has been hypothesized to be the cause of waddling gait [25]. Recent gait analysis in subjects with XLH has found that waddling gait was correlated to varus limb alignment [14] and degenerated hip, knee and ankle joints and enthesopathy of the hip abductors [8]. Lower femoral torsion and high acetabular coverage, both confirmed risk factors of hip osteoarthritis [26], impede hip internal rotation in XLH [8, 40] which results in enhanced risk of femoro-acetabular hip impingement and consecutive joint pain [7, 10]. The lower femoral torsion also increases the shear forces on the femoral neck [11]; this could contribute to development of coxa vara which is common in this population. Tibial torsion also contributes to altered gait as identified in paediatric populations with XLH [14].

Corrective surgery is a common practice in individuals with XLH, with > 57% of adults with XLH and frontal plane deformities [7, 24, 25] having already undergone at least one procedure. In the analysis presented here, the average femorotibial angle was similar in both groups. While this finding appears to conflict with the common perception of XLH being associated with varus deformity of the leg axis, it most likely reflects that all but one subject in the XLH cohort

evaluated here have undergone femoral osteotomies which are usually aimed at correction of frontal plane deformities [24]. In addition, the average mechanical valgus angle was actually increased in the XLH group as compared to controls, along with an increased femoral mechanical–anatomical angle, reflective of an enhanced femoral offset and further supporting this perception, while this aspect of previous corrective osteotomies has to be considered a limitation of our study, otherwise.

However, when planning osteotomies taking into account transverse plane parameters such as regional femoral torsion could be beneficial [41, 42], for example to restore advantageous muscular lever arm length. The restoration of limb alignment in multiple planes could decrease the chances of early arthrosis due to malalignment [43].

To our knowledge, this is the first study to quantitatively characterize multiple objectives and clinically relevant measures of lower-limb bone geometry, in individuals with XLH. Previous studies had reported the incidence of identified deformities such as tibial bowing without a description of the magnitude of deviation or the degree of within-group variance [9, 20].

There are several limitations to this study which have to be kept in mind. Importantly, all statistical analyses and interpretations have to be seen against the background of the limited number of cases for this complex assessment in a rare disorder, and lack of significance in some parameters may be related to the low number of patients enrolled. Furthermore, all but two participants with XLH had corrective surgery on the lower limbs during their lifetime; therefore, observed differences are not solely attributable to differences in natural growth. Indeed, the outcome of corrective interventions and the risk for recurrent deformity or overcorrections are subject to multiple modifiers, including but not limited to surgical technique and performance, age at surgery and quality of accompanying medical treatment. However, considering that it is unethical to let XLH patients grow into adulthood without treating their deformities and understanding limitations regarding availability of data on treatments that occurred 10–50 years ago, real-world data provided here still represent best available evidence. Having said that, data presented here should not be perceived to reflect natural bone development in XLH but rather to provide a real-world inventory of bone deformities in adult XLH patients.

Moreover, the fact that specific differences particularly concerning aspects of rotation and bowing persist even following surgery highlights both the scale of the effects and that different interventional approaches, e.g. pharmacological treatments or physiotherapy/exercise, may be required to comprehensively address this issue. Even though the participants were recruited from a broad clinical cohort, the sample size is small. Therefore, while the observed group differences were large and statistical evidence for them was strong, these findings require replication in a larger cohort. Furthermore, only the left leg was scanned for every subject, as scanning both legs would have quadrupled scanning times. We were therefore unable to assess inter-limb asymmetries, which may contribute to gait and other problems within individuals with XLH. Detailed information on previous pharmacological and other treatments from childhood was not available for all participants, and future studies should examine whether surgical or other treatments impact on bone geometry. Femoral torsion was assessed on two cross-section slices and not on one oblique slice which is now standard practice, while the latter results in slightly smaller torsion values within-population variance is similar [44]; therefore, we believe that this would not substantially impact our main findings. Finally, all frontal plane measurements were assessed using cross-sectional MRIs, and not by the usual clinical method of anteroposterior radiographs.

Conclusions

In conclusion, adults with XLH have substantial differences and greater inter-individual variation in hip and femur bone geometry, principally lower femoral torsion originating in the intertrochanteric region, lower tibial torsion and higher lateral and frontal femoral bowing. Large differences in acetabular coverage and version were also observed, while differences detected between the groups in the mechanical axis and tibiofemoral angle are minimal. These differences are likely to be due to the higher malleability of the bones, variations in gait, delayed motor development and impaired muscle function. These differences were evident despite most individuals within the current study having undergone corrective frontal plane surgery. Accordingly, these observations should be considered when planning corrective surgery in XLH in the future. The presented results have the potential for increased femoral fracture risk and disadvantageous joint mechanics during daily physical activity and could be part of the cause of the osteoarthritis, pain and waddling gait commonly experienced in this clinical group.

Supplementary Information The online version contains supplementary material available at https://doi.org/10.1007/s00198-022-06385-z.

Acknowledgements The authors would like to thank Xaali O'Reilly-Berkeley for the production of original illustrations. In addition, Lorenzo Betti for support in development of the trigonometric formulae.

Funding Open Access funding enabled and organized by Projekt DEAL.

Declarations

Ethics approval Ethical approval for the study was obtained from the competent ethics committees of the medical faculties at the universities of Cologne (no. 19-1020) and Wuerzburg (128/19). The study is registered with the German Register for Clinical Studies (DRKS00016074).

Consent to participate All participants provided written informed consent prior to any study-related procedures.

Conflict of interest MS, SK, JZ, JJ, OS, ES, JR, and AL have no conflict of interest to disclose. LS has received funding from Kyowa Kirin GmbH to support parts of this research.

References

1. Beck-Nielsen SS, Brock-Jacobsen B, Gram J, Brixen K, Jensen TK (2009) Incidence and prevalence of nutritional and hereditary rickets in southern Denmark. Eur J Endocrinol 160:491–497
2. Francis F, Hennig S, Korn B, Reinhardt R, De Jong P, Poustka A, Lehrach H, Rowe P, Goulding J, Summerfield T (1995) A gene (PEX) with homologies to endopeptidases is mutated in patients with X–linked hypophosphatemic rickets. Nat Genet 11:130–136
3. Gaucher C, Walrant-Debray O, Nguyen TM, Esterle L, Garabedian M, Jehan F (2009) PHEX analysis in 118 pedigrees reveals new genetic clues in hypophosphatemic rickets. Hum Genet 125:401–411
4. Carpenter TO (1997) New perspectives on the biology and treatment of X-linked hypophosphatemic rickets. Pediatr Clin 44:443–466
5. Beck-Nielsen SS, Mughal Z, Haffner D, Nilsson O, Levtchenko E, Ariceta G, de Lucas CC, Schnabel D, Jandhyala R, Mäkitie O (2019) FGF23 and its role in X-linked hypophosphatemia-related morbidity. Orphanet J Rare Dis 14:58
6. Lambert AS, Zhukouskaya V, Rothenbuhler A, Linglart A (2019) X-linked hypophosphatemia: Management and treatment prospects. Joint Bone Spine 86:731–738
7. Carpenter TO, Imel EA, Holm IA, Jan de Beur SM, Insogna KL (2011) A clinician's guide to X-linked hypophosphatemia. J Bone Miner Res 26:1381–1388
8. Steele A, Gonzalez R, Garbalosa JC, Steigbigel K, Grgurich T, Parisi EJ, Feinn RS, Tommasini SM, Macica CM (2020) Osteoarthritis, osteophytes, and enthesophytes affect biomechanical function in adults with X-linked hypophosphatemia. J Clin Endocrinol Metab 105:e1798–e1814
9. Skrinar A, Dvorak-Ewell M, Evins A, Macica C, Linglart A, Imel EA, Theodore-Oklota C, San Martin J (2019) The lifelong impact of X-linked hypophosphatemia: results from a burden of disease survey. J Endocrine Soc 3:1321–1334
10. Seefried L, Dahir K, Petryk A, Högler W, Linglart A, Martos-Moreno GÁ, Ozono K, Fang S, Rockman-Greenberg C, Kishnani PS (2020) Burden of illness in adults with hypophosphatasia: data from the global hypophosphatasia patient registry. J Bone Miner Res 35:2171–2178
11. Pritchett JW, Perdue KD (1988) Mechanical factors in slipped capital femoral epiphysis. J Pediatr Orthop 8:385–388
12. Genest F, Seefried L (2018) Subtrochanteric and diaphyseal femoral fractures in hypophosphatasia—not atypical at all. Osteoporos Int 29:1815–1825
13. Scorcelletti M, Reeves ND, Rittweger J, Ireland A (2020) Femoral anteversion: significance and measurement. J Anat 237:811–826
14. Mindler GT, Kranzl A, Stauffer A, Haeusler G, Ganger R, Raimann A (2020) Disease-specific gait deviations in pediatric patients with X-linked hypophosphatemia. Gait Posture 81:78–84
15. Linglart A, Biosse-Duplan M, Briot K, Chaussain C, Esterle L, Guillaume-Czitrom S, Kamenicky P, Nevoux J, Prié D, Rothenbuhler A (2014) Therapeutic management of hypophosphatemic rickets from infancy to adulthood. Endocr Connect 3:R13–R30
16. Zhukouskaya VV, Rothenbuhler A, Colao A, Di Somma C, Kamenický P, Trabado S, Prié D, Audrain C, Barosi A, Kyheng C (2020) Increased prevalence of overweight and obesity in children with X-linked hypophosphatemia. Endocr Connect 9:144–153
17. Bobroff ED, Chambers HG, Sartoris DJ, Wyatt MP, Sutherland DH (1999) Femoral anteversion and neck-shaft angle in children with cerebral palsy. Clin Orthop Relat Res 364:194–204
18. Galbraith RT, Gelberman RH, Hajek PC, Baker LA, Sartoris DJ, Rab GT, Cohen MS, Griffin PP (1987) Obesity and decreased femoral anteversion in adolescence. J Orthop Res 5:523–528
19. Castaño-Betancourt MC, Van Meurs JB, Bierma-Zeinstra S, Rivadeneira F, Hofman A, Weinans H, Uitterlinden AG, Waarsing JH (2013) The contribution of hip geometry to the prediction of hip osteoarthritis. Osteoarthritis Cartilage 21:1530–1536
20. Capelli S, Donghi V, Maruca K, Vezzoli G, Corbetta S, Brandi ML, Mora S, Weber G (2015) Clinical and molecular heterogeneity in a large series of patients with hypophosphatemic rickets. Bone 79:143–149
21. Koo TK, Li MY (2016) A guideline of selecting and reporting intraclass correlation coefficients for reliability research. J Chiropr Med 15:155–163
22. Kim HY, Lee SK, Lee NK, Choy WS (2012) An anatomical measurement of medial femoral torsion. J Pediatric Orthopaedics B 21:552–557
23. Sharkey MS, Grunseich K, Carpenter TO (2015) Contemporary medical and surgical management of X-linked hypophosphatemic rickets. JAAOS-J Am Acad Orthop Surg 23:433–442
24. Gizard A, Rothenbuhler A, Pejin Z, Finidori G, Glorion C, de Billy B, Linglart A, Wicart P (2017) Outcomes of orthopedic surgery in a cohort of 49 patients with X-linked hypophosphatemic rickets (XLHR). Endocr Connect 6:566–573
25. Horn A, Wright J, Bockenhauer D, Van't Hoff W, Eastwood D (2017) The orthopaedic management of lower limb deformity in hypophosphataemic rickets. J Child Orthop 11:298–305
26. Zeng W-N, Wang F-Y, Chen C, Zhang Y, Gong X-Y, Zhou K, Chen Z, Wang D, Zhou Z-K, Yang L (2016) Investigation of association between hip morphology and prevalence of osteoarthritis. Sci Rep 6:23477
27. León-Muñoz VJ, Manca S, López-López M, Martínez-Martínez F, Santonja-Medina F (2021) Coronal and axial alignment relationship in Caucasian patients with osteoarthritis of the knee. Sci Rep 11:1–8
28. Insogna KL, Briot K, Imel EA, Kamenický P, Ruppe MD, Portale AA, Weber T, Pitukcheewanont P, Cheong HI, Jan de Beur S (2018) A randomized, double-blind, placebo-controlled, phase

3 trial evaluating the efficacy of burosumab, an anti-FGF23 antibody, in adults with X-linked hypophosphatemia: week 24 primary analysis. J Bone Miner Res 33:1383–1393
29. Haffner D, Emma F, Eastwood DM, Duplan MB, Bacchetta J, Schnabel D, Wicart P, Bockenhauer D, Santos F, Levtchenko E (2019) Clinical practice recommendations for the diagnosis and management of X-linked hypophosphataemia. Nat Rev Nephrol 15:435–455
30. Veilleux L-N, Cheung MS, Glorieux FH, Rauch F (2013) The muscle-bone relationship in X-linked hypophosphatemic rickets. J Clin Endocrinol Metab 98:E990–E995
31. Hadjab I, Farlay D, Crozier P, Douillard T, Boivin G, Chevalier J, Meille S, Follet H (2021) Intrinsic properties of osteomalacia bone evaluated by nanoindentation and FTIRM analysis. J Biomech 117:110247
32. Veilleux NJ, Kalore NV, Wegelin JA, Vossen JA, Jiranek WA, Wayne JS (2018) Automated femoral version estimation without the distal femur. J Orthop Res 36:3161–3168
33. Ireland A, Rittweger J, Schönau E, Lamberg-Allardt C, Viljakainen H (2014) Time since onset of walking predicts tibial bone strength in early childhood. Bone 68:76–84
34. Ireland A, Saunders FR, Muthuri SG, Pavlova AV, Hardy RJ, Martin KR, Barr RJ, Adams JE, Kuh D, Aspden RM (2019) Age at onset of walking in infancy is associated with hip shape in early old age. J Bone Miner Res 34:455–463
35. Zhang C, Zhao Z, Sun Y, Xu L, JiaJue R, Cui L, Pang Q, Jiang Y, Li M, Wang O (2019) Clinical and genetic analysis in a large Chinese cohort of patients with X-linked hypophosphatemia. Bone 121:212–220
36. Hardy D, Murphy W, Siegel B, Reid I, Whyte M (1989) X-linked hypophosphatemia in adults: prevalence of skeletal radiographic and scintigraphic features. Radiology 171:403–414
37. Portale AA, Carpenter TO, Brandi ML et al (2019) Continued beneficial effects of burosumab in adults with X-linked hypophosphatemia: results from a 24-week treatment continuation period after a 24-week double-blind placebo-controlled period. Calcif Tissue Int 105:271–284
38. Scheys L, Van Campenhout A, Spaepen A, Suetens P, Jonkers I (2008) Personalized MR-based musculoskeletal models compared to rescaled generic models in the presence of increased femoral anteversion: effect on hip moment arm lengths. Gait Posture 28:358–365
39. Li H, Wang Y, Oni J, Qu X, Li T, Zeng Y, Liu F, Zhu Z (2014) The role of femoral neck anteversion in the development of osteoarthritis in dysplastic hips. Bone J J 96:1586–1593
40. Bedi A, Dolan M, Leunig M, Kelly BT (2011) Static and dynamic mechanical causes of hip pain. Arthros J Arthroscop Relate Surg 27:235–251
41. Seitlinger G, Moroder P, Scheurecker G, Hofmann S, Grelsamer RP (2016) The contribution of different femur segments to overall femoral torsion. Am J Sports Med 44:1796–1800
42. Waisbrod G, Schiebel F, Beck M (2017) Abnormal femoral antetorsion-a subtrochanteric deformity. J Hip Preserv Surg 4:153–158
43. Khan FA, Koff MF, Noiseux NO, Bernhardt KA, O'Byrne MM, Larson DR, Amrami KK, Kaufman KR (2008) Effect of local alignment on compartmental patterns of knee osteoarthritis. J Bone J Surg Am 90:1961
44. Sutter R, Dietrich TJ, Zingg PO, Pfirrmann CW (2015) Assessment of femoral antetorsion with MRI: comparison of oblique measurements to standard transverse measurements. Am J Roentgenol 205:130–135